LOS Path Identification in Multipath Environments with an Unknown Number of Passive Targets

Yifan Liang, Cengcang Zeng, and Hongbin Li
Department of Electrical and Computer Engineering
Stevens Institute of Technology
Hoboken, NJ 07030, USA

***Abstract*—This work extends a recently introduced type-based clustering algorithm (TCA) [1] for identifying line-of-sight (LOS) paths in multipath environments with multiple passive targets. In particular, while [1] assumes that the number of targets is known, we consider herein a more practical scenario without the assumption. The system consists of several spatially dispersed sensors, each emitting a unique waveform. These sensors exploit the returned echoes to measure both LOS and non-line-of-sight (NLOS) time delays (or equivalently, ranges) of targets within the observation area. For ease of exposition, we consider a 2-dimensional (2D) localization scenario. In this context, every range estimate represents a circle, and combining measurements from different sensors produces intersection points on the plane. By applying TCA and examining the structural properties of points created by LOS paths, we categorize the clustered point sets into six possible cases. To estimate the number of targets in presence, we analyze these cases and formulate a discriminant function to identify the sets associated with the targets, thereby enabling us to jointly determine the number of targets and the associated LOS measurements. We present numerical results to showcase the performance of the proposed scheme under various configurations.**

I. Introduction

Localization problems are pivotal in numerous applications, ranging from mobile communication to surveillance and navigation, where there usually exist multiple targets to be located. These problems can broadly be categorized into two main types: active and passive localization. In active localization, each target (e.g. a cellphone) emits a distinct waveform, which is then received by sensors [2]. In such scenarios, unique waveforms produced by different targets serve as identifying signatures, allowing the active localization system to distinguish among multiple targets as effectively as it does with a single target. The ability of sensors to detect these unique waveforms provides an estimate of the target count within the environment, mitigating the complexity typically associated with multi-target localization. In contrast, passive localization relies on an external radio transmitter to illuminate targets (e.g. people), and the ensuing reflected echoes are used for the target localization. Passive settings present added complexities, notably in multipath settings with several targets [3], [4]. One significant challenge arises due to all targets reflecting an identical waveform upon the same illumination. This can lead to scenarios where a non-line-of-sight (NLOS) echo from one target might be mistaken for a line-of-sight (LOS) echo from another, complicating the task of determining the accurate location of targets and the number of targets present.

A linchpin in the localization problem is the reliance on LOS paths to discern target locations [5]. In the absence of prior knowledge on NLOS measurements, such as the potential scatterers' positions, NLOS paths introduce inevitable positive biases in localization estimates [2], [5]. The research community has delved deep into LOS detection methodologies for both active and passive localization cases [5], spanning hypothesis testing [6], [7] and nonparametric techniques [8], [9]. However, a majority of these methods were tailored predominantly for active single-target localization in multipath environments, rendering them suboptimal for passive multi-target settings. The LOS identification problem for passive multi-target localization was recently addressed in [1], where a type-based clustering algorithm (TCA) was proposed. However, this method requires the prior knowledge of the number of targets to be detected, a prerequisite that may limit its applicability in practice.

This work extends the original TCA algorithm by leveraging the inherent characteristics to classify and screen the search results, thereby eliminating the dependence on prior knowledge of the number of targets. Specifically, the LOS identification process is integrated with a joint estimation process for the target number, which exploits some inherent properties related to the intersection points, such as uniqueness and spread of point sets. Simulation results indicate that the extended TCA is capable of reliably identifying the number of targets as well as their associated LOS measurements, especially when the range measurements are relatively accurate. We further discuss the influence of different setups on the performance of the extended TCA. Numerical simulations show that the extended TCA leads to accurate location estimates for the passive multi-target localization problem.

II. Signal Model

Consider there are N sensor nodes located at coordinates $\mathbf{a}_n \in \mathbb{R}^2$, with n ranging from 1 to N. The network is tasked with finding the positions of K unknown targets at locations $\mathbf{p}_k \in \mathbb{R}^2$, where k varies from 1 to K. Additionally, the environment contains L non-target scattering objects situated at coordinates $\mathbf{s}_l \in \mathbb{R}^2$, with l ranging from 1 to L. Each

This work was supported in part by the National Science Foundation under grants CCF-2316865, ECCS-1923739, ECCS-2212940, and ECCS-2332534.

sensor in the network performs a scan of its surroundings by emitting a unique waveform. It then calculates the time delays of echoes returned from targets and scatterers using a matched filter [2]. These time-delay measurements are converted into *range* observations. The distinction among the two types of measurements, LOS and NLOS, is in general unknown a priori. Mathematically, these observations can be represented as follows:

$$\begin{cases} r_{n,k} = \|\mathbf{p}_k - \mathbf{a}_n\| + \epsilon_{n,k}, \\ y_{n,k,l} = \|\mathbf{p}_k - \mathbf{a}_n\| + \|\mathbf{p}_k - \mathbf{s}_l\| + \|\mathbf{s}_l - \mathbf{a}_n\| + \epsilon_{n,k,l}, \end{cases} \tag{1}$$

where ϵ signifies zero-mean range measurement noise with a variance of σ^2, and $r_{n,k}$ denotes the LOS range measurement from sensor n to target k. $y_{n,k,l}$ represents NLOS range observation from sensor n to target k, scattered via scatterer l. Considering the reversibility of light paths, the NLOS path measurements remain identical whether the signal first encounters the scatterer or the target. Therefore, we only consider one of these scenarios for our range measurements.

One critical challenge faced by such a multi-sensor localization system is its inability to differentiate between LOS measurements $r_{n,k}$ and NLOS measurements $y_{n,k,l}$. It also struggles with attributing each measurement to its corresponding target, especially when an unknown number of targets is present. Therefore, the primary focus of this work is the development of a computational algorithm capable of determining the number of targets in the environment and identifying the LOS measurements $r_{n,k}$ for each individual target by leveraging the inherent geometric patterns present in the collected data.

III. Proposed Algorithm

A. Overview of TCA

TCA originates from a fact that any specific range measurement obtained by a sensor can be represented as a circle centered at that sensor, with the measured range as its radius. The circles corresponding to LOS range measurements are called *LOS circles*, while the NLOS ones are called *NLOS circles*.

In practice, although measurement noise affects the accuracy and causes the LOS circles to deviate from the perfect intersection at the target, a distinct geometric pattern still emerges. Fig. 1 illustrates the geometric representation of range measurements with noise. In the example, three LOS circles produce three intersection points, $p_{1,2}$, $p_{1,3}$ and $p_{2,3}$, spread around the target in the center. These points are called *target intersection points (TIPs)*. Such a collection of points consisting of intersections of the LOS circles is called a TIP set of the target in the center.

The fundamental LOS identification problem of interest is to identify the TIP set of each target from numerous intersection points produced by LOS and NLOS circles, which is challenging in practice. In [1], TCA was proposed for the TIP set identification problem by exploiting the inherent properties of TIP sets. It assumes that the number of targets

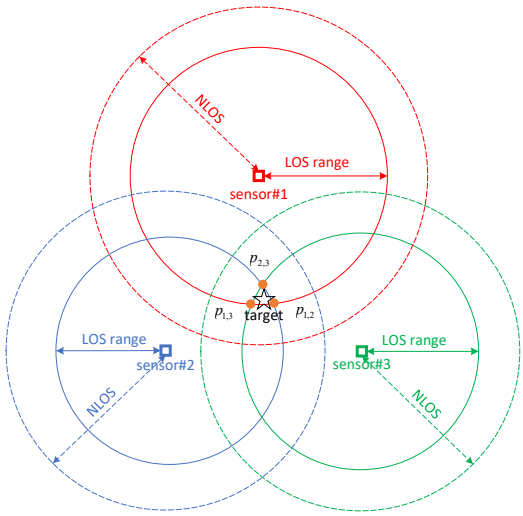

Figure 1. Illustration of $N = 3$ LOS circles respectively centered at 3 sensors (denoted by red, blue, and green squares). A TIP set is produced by these LOS circles around the true target location. Points $p_{1,2}$, $p_{1,3}$ and $p_{2,3}$ are TIPs.

K is known in advance, while prior knowledge about the number of targets is usually lacking in practice. In this work, we address this problem by extending TCA to incorporate the joint estimation of the number of targets.

B. Extending TCA with Joint Estimation of K

The extended TCA builds upon a foundational two-stage search process of its predecessor by introducing an improved final screening phase. The 2-stage search is developed from several concepts explained next. The set of circles centered at the n-th sensor is called a *circle set*, denoted by $\mathcal{C}_n$, and the set of intersection points produced by two different circle sets is defined as a *type* set of type (n_1, n_2):

$$\begin{aligned} \mathcal{T}_{n_1,n_2} &\triangleq \{x \in \mathbb{R}^2 | x = \mathcal{C}_{n_1} \cap \mathcal{C}_{n_2}\} \\ n_1 = 1, \ldots, N-1, n_2 &= 2, \ldots, N, n_1 < n_2. \end{aligned} \tag{2}$$

The 2-stage search process aims to search for a number of *structured candidate sets*. Each structured candidate set given by the 2-stage search, denoted as $\mathcal{U}_j^{N(N-1)/2}$. The subscript of such a notation means that the set contains $N(N-1)/2$ points from $N(N-1)/2$ different types. These structured candidate sets can be classified into 6 cases, as illustrated in Fig. 2 assuming $N = 3$ sensors. Note that the classification holds for arbitrary $N \geq 3$, and the illustration uses $N = 3$ for simplicity. Specifically, Case (i) represents a TIP set, while Cases (ii)-(vi) represent the five possible cases of non-TIP sets. Cases (ii) and (iii) are the *structured candidate sets* that contain *at least* one TIP but not all TIPs. The difference between Cases (ii) and (iii) is that (ii) is produced by only LOS circles while (iii) by both LOS and NLOS circles. Cases (iv), (v), and (vi) are the three possible cases that do not contain any TIPs, among which (iv) is produced by only LOS circles, (v) by both LOS and NLOS circles, and (vi) by only NLOS circles. Since each point on the plane is produced by a pair of intersecting circles,

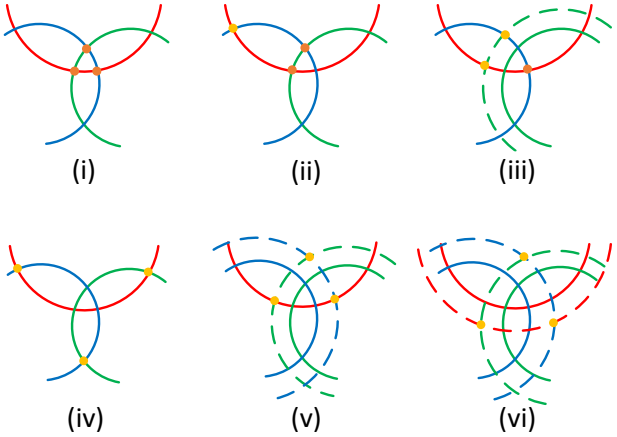

Figure 2. Illustration of the six possible cases of structured candidate sets when $N = 3$. Solid arcs represent LOS circles and dashed arcs NLOS circles.

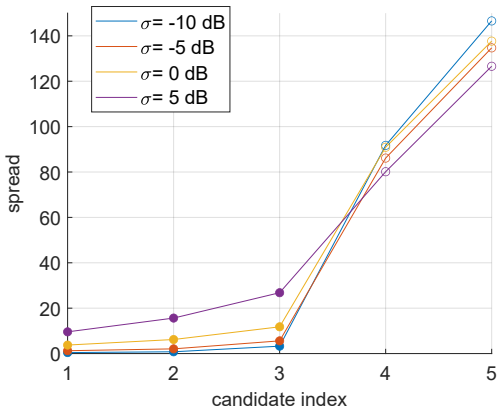

Figure 3. Average spread of the first 5 candidates given by TCA over 300 independent simulations with $N = 5$, $K = 3$, and $L = 4$. The filled circles represent the spread of K TIP sets and the hollow circles denote the spread of 2 following structured candidate sets.

the *parent set* of a point set $\mathcal{U}^m$ is defined as the set of all circles that involve producing the point set $\mathcal{U}^m$, denoted by $\mathcal{P}(\mathcal{U}^m)$. Moreover, the *spread* of a point set $\mathcal{U}^m$, denoted by $s(\mathcal{U}^m)$, is defined to describe the dispersion of the set

$$s(\mathcal{U}^m) = \sqrt{\sum_{i=1}^{m}(x_i - \bar{x})^2 + (y_i - \bar{y})^2} \tag{3}$$

where x_i, y_i represent the x-coordinate and $y-$coordinate of the i-th point in the set, and $\bar{x}$ and $\bar{y}$ are, respectively, the means of the x-coordinates and y-coordinates of the points.

Different from [1], the final screening process integrates the joint estimation of K and TIP set identification as elaborated next. Since there exists a one-to-one mapping between TIP sets and the targets to be localized in the environment, the estimation of K can be transformed into the estimation towards the number of TIP sets, i.e. the number of Case (i). Note the above classification can be leveraged to differentiate Case (i) from the other Cases. Firstly, we explain how to differentiate Cases (ii) and (iii) from (i). A candidate point set $\mathcal{U}_j^{N(N-1)/2}$ is considered *unique* if

$$\mathcal{U}_j^{N(N-1)/2} \cap \mathcal{V}_k = \emptyset, k = 1, \ldots, K \tag{4}$$

where $\mathcal{V}_k$ denotes a TIP set. Otherwise, the candidate set is considered *non-unique*. It is noted that (ii) and (iii) are both non-unique with respect to the corresponding TIP set. Although the TIP set is unknown in practice, the final screening process is designed to compare all non-unique candidate sets with each other and, in each comparison, only preserve the candidate set with a smaller spread. The comparison is finished if for any two different $\mathcal{U}_i^{N(N-1)/2}$ and $\mathcal{U}_j^{N(N-1)/2}$ among the remaining candidate sets, we have

$$\mathcal{U}_i^{N(N-1)/2} \cap \mathcal{U}_j^{N(N-1)/2} = \emptyset. \tag{5}$$

As shown in Fig. 2, the spread of Case (i) is usually smaller than the spread of the non-unique candidate sets of (ii) and (iii). Therefore, Cases (ii) and (iii) can be eliminated from the candidate sets while case (i) is preserved by the above uniqueness-based comparison.

We now discuss how to differentiate Cases (iv)-(vi) from (i) among the remaining candidate sets. The uniqueness-based comparison *cannot* eliminate Cases (iv)-(vi) since these candidate sets are unique and thus satisfy the condition (5). Note as shown in Fig. 2, the spread of Cases (iv)-(vi) is generally larger than that of Case (i). Considering a setup with $N = 5$ sensors, $K = 3$ targets, and $L = 4$ NLOS scatterers, Fig. 3 shows the spread of reordered structured candidate sets (in the order of ascending spread), after removing Cases (ii) and (iii). The figure clearly exhibits an *"elbow"* when the index exceeds the target number K. The results indicate that even with the highest noise level $\sigma = 5$ dB, the average spread of each TIP set is still significantly smaller than that of the structured candidate sets of Cases (iv)-(vi).

Hence, we can use the elbow feature to estimate the target number K. Specifically, the remaining structured candidate sets, after removing Cases (ii) and (iii) as mentioned above, are ordered based on their spread. Let S^* contain the resulting structured candidate sets in non-decreasing order of spread, which are denoted by

$$S^* = \{\mathcal{U}_1^*, \mathcal{U}_2^* \ldots, \mathcal{U}_{K_c}^*\} \tag{6}$$

where $K_c = |S^*|$ and assume $K_c > K$. The spread of the k-th candidate set is expressed as $s(\mathcal{U}_k^*)$. Define the *spread difference function*

$$d(\mathcal{U}_k^*) \triangleq s(\mathcal{U}_{k+1}^*) - \frac{\sum_{q=1}^{k} s(\mathcal{U}_q^*)}{k}, k = 1, \ldots, K_c - 1. \tag{7}$$

We calculate $d(\mathcal{U}_k^*)$ starting from $k = 1$. For the $\hat{K}$-th candidate set, if $d(\mathcal{U}_{\hat{K}}^*)$ is larger than η, referred to as the *elbow threshold*, then $\hat{K}$ represents an estimate of the number of targets in the environment. Otherwise, continue the calculation with the next candidate set.

Consequently, the extended TCA does not require any prior

knowledge of the target number to give $\hat{K}$ estimates of TIP sets $\hat{\mathcal{U}}_1^*, \ldots, \hat{\mathcal{U}}_{\hat{K}}^*$. For each output set $\hat{\mathcal{U}}_j^*$, $|\mathcal{P}(\hat{\mathcal{U}}_j^*)| = N$ is guaranteed, i.e. the parent set of $\hat{\mathcal{U}}_j^*$ consists of N circles which are respectively centered at a specific sensor. The radii of these circles, denoted by $\hat{r}_{n,j}, n = 1, \ldots, N$, represent estimates of the LOS range measurements $r_{n,k}$ in (1).

C. Target Localization

With the obtained LOS measurements corresponding to the $\hat{K}$ targets, the multi-target localization problem is converted into localization problems of several single targets, which can be solved by existing methods, such as the *range-based least squares* (R-LS) estimator and the *squared-range-based least squares* (SR-LS) estimator [10]

$$\text{(R-LS)}: \quad \min_{\mathbf{p}_j} \sum_{n=1}^{N} \left(\hat{r}_{n,j} - \|\mathbf{p}_j - \mathbf{a}_n\|\right)^2 \tag{8}$$

$$\text{(SR-LS)}: \quad \min_{\mathbf{p}_j} \sum_{n=1}^{N} \left(\hat{r}_{n,j}^2 - \|\mathbf{p}_j - \mathbf{a}_n\|^2\right)^2 \tag{9}$$

where $j = 1, \ldots, \hat{K}$. R-LS provides with better localization accuracy among the two since it is optimal in the maximum likelihood sense. R-LS can be solved by using the iterative Nelder-Mead method or grid search. Such methods require an initial point to start searching for the optimal solution on the plane. We use the SR-LS solution (9) as the initial point since SR-LS can be solved efficiently as demonstrated in [10]. Simulation results verified that the global optimum for (8) is always available in this way.

IV. Simulation Results

Numerical results are presented to demonstrate the performance of the extended TCA in various scenarios. We consider a 400×400 square surveillance region with its center at the origin $(0, 0)$. N sensors are evenly placed along a circle also centered at the origin with a radius of 160. $L = 3$ scatterers are randomly positioned along the square's perimeter. While the positions of both sensors and scatterers remain fixed throughout the simulations, $K = 3$ targets are randomly generated in different trial runs. The measurement noise, being independent across observations, follows a Gaussian distribution with a mean of zero and a variance denoted by σ^2. In this work, noise level is described in dB ($10\log_{10}(\sigma)$).

We first examine the impact of noise, N (the number of sensors), and the elbow threshold η on estimating the target number K. The stacked bar graphs in Fig.4 show the probability of different estimations in different setups. Note that $\hat{K} = 1$ and $\hat{K} = 2$ represent the cases where TCA underestimates the true number $K = 3$, while $\hat{K} = 4$ and $\hat{K} \geq 5$ correspond to the cases where the extended TCA overestimates K. Simulation results show that our proposed algorithm provides with a reliable probability of correctly estimating the target number by choosing a proper spread threshold η under different setups. With more sensors (i.e. larger N), a larger η is able to provide with better estimation reliability. For example, when $N = 4$, the extended TCA with $\eta = 15$ has higher probability (by $8\% \sim 12\%$) of correctly estimating K than that with $\eta = 35$. When N is increased to 6, the extended TCA with $\eta = 35$ outperforms that with $\eta = 15$ and has a 100% probability of correct target number estimation for $\sigma = 0$dB, 99.6% for $\sigma = 2.5$dB, and 97.9% for $\sigma = 5$dB.

Moreover, we demonstrate the LOS identification accuracy of the extended TCA. Table.I and II exhibit the number of trails (out of 1000 independent simulations) where true LOS measurements are correctly identified by the extended TCA. With a relatively large $\sigma = 0$dB, our proposed algorithm still provides at least a more than 71% probability of correct identification (except 67.1% with $N = 4$ and $\eta = 35$). The results underscore the reliability of our proposed algorithm in LOS identification across low to medium noise levels. Although the LOS identification becomes inevitably more challenging with the increasing noise level as shown in the tables, our proposed algorithm still behaves well in the estimation of the number of TIP sets on the plane, i.e. targets. This leads to an outstanding localization accuracy by using R-LS along with SR-LS estimates (8)(9) for such passive multi-target localization problems [1].

V. Conclusion

In this work, we developed the extended TCA by leveraging the inherent properties of the search sets from the original TCA algorithm, classifying them into six cases. Then we design two mechanisms, the uniqueness-based comparison and the elbow feature, based on the distinct characteristics of these cases to accomplish the estimation of the number of targets. Simulation results show that in the considered range of noise level from -10dB to 5dB, our proposed algorithm provides a good performance on both target number estimation and LOS identification, by setting up a proper threshold η in the algorithm. Such observations verify that the proposed work leads to a solution of the passive multi-target localization problem with good accuracy.

References

[1] Y. Liang and H. Li, "LOS signal identification for passive multi-target localization in multipath environments," *IEEE Signal Processing Letters*, vol. 30, pp. 1597–1601, 2023.

[2] S. Gezici, Z. Tian, G. Giannakis, H. Kobayashi, A. Molisch, H. Poor, and Z. Sahinoglu, "Localization via ultra-wideband radios: a look at positioning aspects for future sensor networks," *IEEE Signal Processing Magazine*, vol. 22, no. 4, pp. 70–84, 2005.

[3] F. Wang, H. Li, X. Zhang, and B. Himed, "Signal parameter estimation for passive bistatic radar with waveform correlation exploitation," *IEEE Transactions on Aerospace and Electronic Systems*, vol. 54, no. 3, pp. 1135–1150, 2017.

[4] X. Zhang, F. Wang, H. Li, and B. Himed, "Maximum likelihood and IRLS based moving source localization with distributed sensors," *IEEE Transactions on Aerospace and Electronic Systems*, vol. 57, no. 1, pp. 448–461, 2020.

[5] S. Aditya, A. F. Molisch, and H. M. Behairy, "A survey on the impact of multipath on wideband time-of-arrival based localization," *Proceedings of the IEEE*, vol. 106, no. 7, pp. 1183–1203, 2018.

[6] İ. Güvenç, C.-C. Chong, F. Watanabe, and H. Inamura, "NLOS identification and weighted least-squares localization for UWB systems using multipath channel statistics," *EURASIP Journal on Advances in Signal Processing*, vol. 2008, pp. 1–14, 2007.

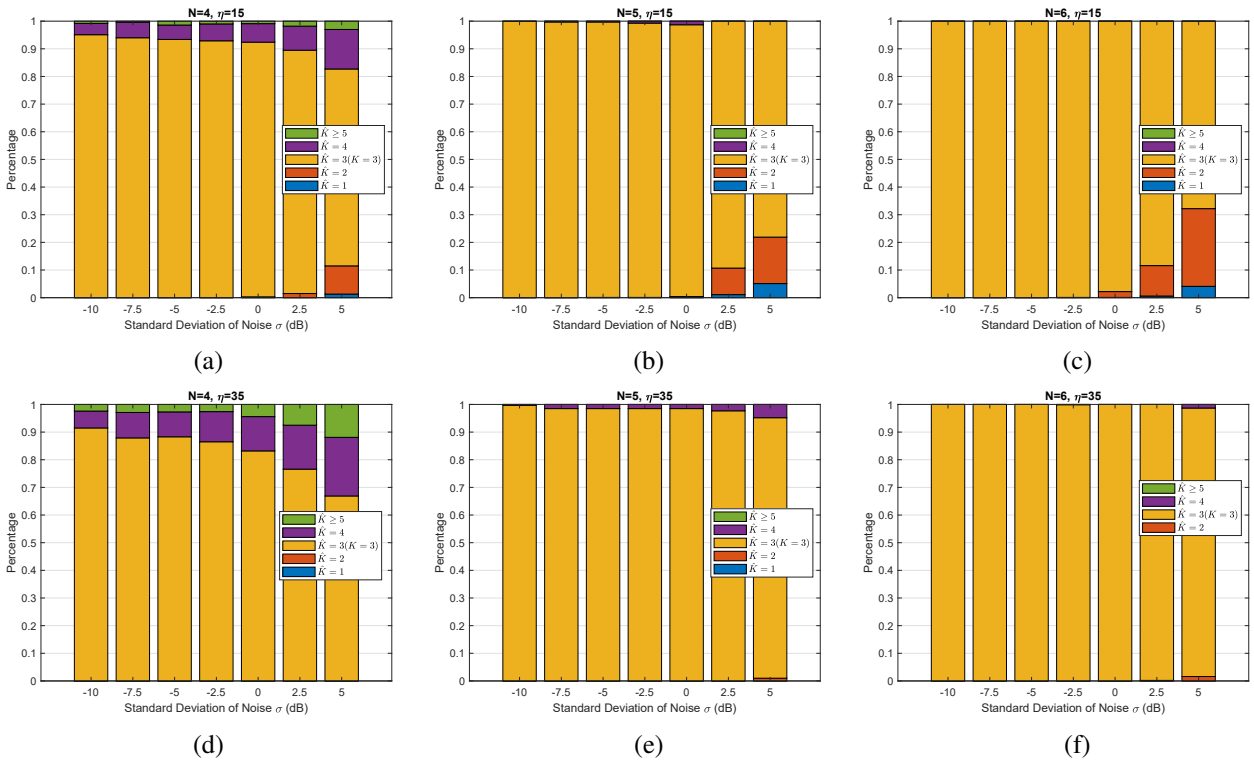

Figure 4. Estimation of target number versus σ with different numbers of sensors N, when the *elbow threshold* $\eta = 15$ (upper row) and $\eta = 35$ (lower row). Since the target number estimate $\hat{K}$ varies across different trials, the probability of a specific value of $\hat{K}$ over all trials is represented by the corresponding color bar height.

Table I
PERFORMANCE OF THE EXTENDED TCA WITH $\eta = 15$

N	**-10dB**	**-7.5dB**	**-5dB**	**-2.5dB**	**0dB**	**2.5dB**	**5dB**
4	923	917	868	828	755	667	444
5	972	955	927	875	758	584	336
6	983	963	886	840	710	481	295

Table II
PERFORMANCE OF THE EXTENDED TCA WITH $\eta = 35$

N	**-10dB**	**-7.5dB**	**-5dB**	**-2.5dB**	**0dB**	**2.5dB**	**5dB**
4	888	856	822	771	671	570	400
5	970	943	916	868	757	647	437
6	983	963	886	840	727	550	422

[7] A. Conti, M. Guerra, D. Dardari, N. Decarli, and M. Z. Win, "Network experimentation for cooperative localization," *IEEE Journal on Selected Areas in Communications*, vol. 30, no. 2, pp. 467–475, 2012.

[8] N. Decarli, D. Dardari, S. Gezici, and A. A. D'Amico, "LOS/NLOS detection for UWB signals: A comparative study using experimental data," in *IEEE 5th International Symposium on Wireless Pervasive Computing 2010*. IEEE, 2010, pp. 169–173.

[9] S. Marano, W. M. Gifford, H. Wymeersch, and M. Z. Win, "NLOS identification and mitigation for localization based on UWB experimental data," *IEEE Journal on selected areas in communications*, vol. 28, no. 7, pp. 1026–1035, 2010.

[10] A. Beck, P. Stoica, and J. Li, "Exact and approximate solutions of source localization problems," *IEEE Transactions on Signal Processing*, vol. 56, no. 5, pp. 1770–1778, 2008.